AFRL-VA-WP-TR-2005-3001

IMPROVED METHODOLOGY FOR ADVANCED AIRCRAFT DESIGN

William A. Crossley

Purdue University
School of Aeronautics and Astronautics
West Lafayette, IN 47907-2023

SEPTEMBER 2004

Final Report for 29 September 2000 – 31 May 2004

STINFO FINAL REPORT

AIR VEHICLES DIRECTORATE
AIR FORCE MATERIEL COMMAND
AIR FORCE RESEARCH LABORATORY
WRIGHT-PATTERSON AIR FORCE BASE, OH 45433-7542

NOTICE

Using Government drawings, specifications, or other data included in this document for any purpose other than Government procurement does not in any way obligate the U.S. Government. The fact that the Government formulated or supplied the drawings, specifications, or other data does not license the holder or any other person or corporation; or convey any rights or permission to manufacture, use, or sell any patented invention that may relate to them.

This report has been reviewed and is releasable to the National Technical Information Service (NTIS). It will be available to the general public, including foreign nationals.

This technical report has been reviewed and is approved for publication.

/s/
_____

MAXWELL BLAIR
Aerospace Engineer
Design & Analysis Methods Branch
Structures Division

/s/
_____

MICHAEL L. ZEIGLER
Chief
Design & Analysis Methods Branch
Structures Division

/s/
_____

JOHN A. BOWLUS
Chief, Structures Division
Air Vehicles Directorate

This report is published in the interest of scientific and technical information exchange and does not constitute approval or disapproval of its ideas or findings.

	REPORT DOCUMENTATION PAGE			Form Approved OMB No. 0704-0188

The public reporting burden for this collection of information is estimated to average 1 hour per response, including the time for reviewing instructions, searching existing data sources, searching existing data sources, gathering and maintaining the data needed, and completing and reviewing the collection of information. Send comments regarding this burden estimate or any other aspect of this collection of information, including suggestions for reducing this burden, to Department of Defense, Washington Headquarters Services, Directorate for Information Operations and Reports (0704-0188), 1215 Jefferson Davis Highway, Suite 1204, Arlington, VA 22202-4302. Respondents should be aware that notwithstanding any other provision of law, no person shall be subject to any penalty for failing to comply with a collection of information if it does not display a currently valid OMB control number. **PLEASE DO NOT RETURN YOUR FORM TO THE ABOVE ADDRESS**.

1. REPORT DATE *(DD-MM-YY)*	2. REPORT TYPE		3. DATES COVERED *(From - To)*
September 2004	Final		09/29/2000 – 05/31/2004

4. TITLE AND SUBTITLE	5a. CONTRACT NUMBER
IMPROVED METHODOLOGY FOR ADVANCED AIRCRAFT DESIGN	F33615-00-C-3051
	5b. GRANT NUMBER
	5c. PROGRAM ELEMENT NUMBER 0601102

6. AUTHOR(S)	5d. PROJECT NUMBER
William A. Crossley	A08D
	5e. TASK NUMBER
	5f. WORK UNIT NUMBER 0B

7. PERFORMING ORGANIZATION NAME(S) AND ADDRESS(ES)	8. PERFORMING ORGANIZATION REPORT NUMBER
Purdue University School of Aeronautics and Astronautics West Lafayette, IN 47907-2023	

9. SPONSORING/MONITORING AGENCY NAME(S) AND ADDRESS(ES)	10. SPONSORING/MONITORING AGENCY ACRONYM(S)
Air Vehicles Directorate Air Force Research Laboratory Air Force Materiel Command Wright-Patterson Air Force Base, OH 45433-7542	AFRL/VASD
	11. SPONSORING/MONITORING AGENCY REPORT NUMBER(S) AFRL-VA-WP-TR-2005-3001

12. DISTRIBUTION/AVAILABILITY STATEMENT
Approved for public release; distribution is unlimited.

13. SUPPLEMENTARY NOTES
Report contains color.

14. ABSTRACT

A set of related topics address aircraft that are significantly different from traditional aircraft. All of the effort relied upon multidisciplinary analysis tools, including finite element modeling, computational aerodynamic prediction, and aeroelastic analysis. An initial investigation focused upon aeroelastic modeling and related design approaches for joined-wing aircraft. Subsequent investigations focused upon design approaches for morphing aircraft.

15. SUBJECT TERMS
Aircraft, Design, Aeroelasticity, Optimization, Morphing, Joined-Wing, Adaptive Structures

16. SECURITY CLASSIFICATION OF:			17. LIMITATION OF ABSTRACT:	18. NUMBER OF PAGES	19a. NAME OF RESPONSIBLE PERSON (Monitor)
a. REPORT Unclassified	b. ABSTRACT Unclassified	c. THIS PAGE Unclassified	SAR	36	Maxwell Blair 19b. TELEPHONE NUMBER *(Include Area Code)* (937) 255-8430

Standard Form 298 (Rev. 8-98)
Prescribed by ANSI Std. Z39-18

TABLE OF CONTENTS

OVERVIEW

The effort conducted under contract F33615-00-C-3051 "Improved Methodology for Advanced Aircraft Design" investigated several topics over a three and a half year period. These topics all related to aircraft concepts and / or configuration that are significantly different from traditional aircraft. All of the effort relied upon multidisciplinary analysis tools, including finite element modeling, computational aerodynamic prediction, and aeroelastic analyses. Initial investigations focused upon aeroelastic modeling and related design approaches for joined wing aircraft.

Subsequent investigations focused upon design approaches for morphing aircraft. These morphing-related topics included design of wings with conformal trailing edge control surfaces to minimize weight and induced drag, using energy as an objective in the design of morphing aerodynamic shapes (both airfoils and wings), and using aeroelastic / structural optimization to develop a weight predictor for morphing wings.

Several graduate students have been supported under this contract, and, at the end of the period, two MS theses and one PhD thesis were completed. Also at the end of the period, two MS theses and one PhD thesis were still in progress. The effort also supported one post-doctoral researcher.

AEROELASTIC TAILORING AND STRUCTURAL OPTIMIZATION OF JOINED WINGS

In this effort, aeroelastic analyses and wing weight optimization for a joined-wing aircraft configuration were investigated. The aeroelastic features of a joined-wing aircraft were examined using both the Rayleigh-Ritz method and the ASTROS finite element-based aeroelastic stability and weight optimization. The high-fidelity analysis tool employed in this study (ASTROS) allowed the joined-wing concept to be structurally optimized with stress, displacement, cantilever, or body-freedom flutter constraints. A series of Matlab scripts were developed to provide pre- and post-processing of the ASTROS input and output files; this included generation of several different presentations of the resulting designs. Aircraft rigid body modes were included to assess body-freedom flutter of the joined-wing aircraft. Several studies using these approaches highlighted parameters that most strongly affect the aeroelastic behavior for a joined-wing aircraft. Wings using both isotropic and composite materials were evaluated using this approach.

Using the Ritz approximation approach, it was possible to rapidly predict flutter speeds for both wing cantilever flutter and body freedom flutter. Figure 1 below presents the results of an analysis that varies the leading wing sweep (L1) for various values of the fuselage pitching moment of inertia. The Ritz analysis approach indicates that there is a distinct transition between cantilever wing flutter and body-freedom flutter for joined-wing configurations, and body-freedom flutter is the critical instability at low values of fuselage pitching inertia. The effect of the leading wing sweep changes the characteristics of transition between the two flutter modes; as the sweep decreases, the transition occurs at lower speeds and at higher values of fuselage pitch moment of inertia. In the plot, the flutter speed is represented by a non-dimensional dynamic pressure ($\bar{q} = qc_{l_\alpha}c_1e_1L_1^2/(GJ)_1$).
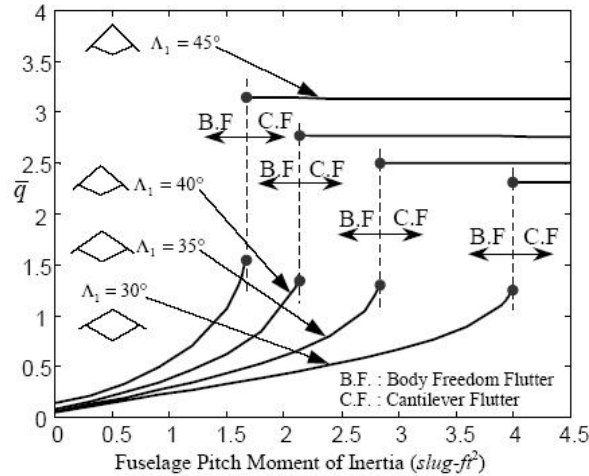

Figure 1 Ritz approximation-based body-freedom to cantilever flutter transition.

Additionally, the relative location of the outboard wing joint can significantly affect this transition between body-freedom and cantilever flutter modes. The position of the wing joint, β, indicates the fraction of forward wing span at which the front and rear wings are joined (i.e. β = 1.0 signifies the joint at the wing tip). Figure 2 presents the body-freedom flutter speed as a function of both leading edge sweep and the joint location. Clearly, the trend presented by this behavior changes in character as the leading wing sweep decreases from 35° to 30°.
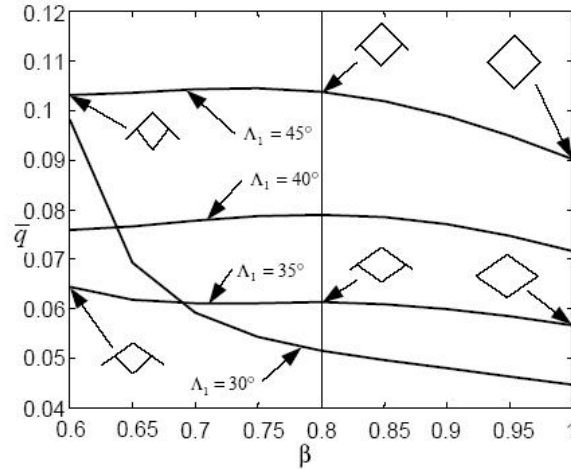
Figure 2 Ritz approximation-based body-freedom flutter speed as a function of leading wing sweep and wing joint location.

Because the Ritz approach indicates that body-freedom flutter is a significant feature of the joined-wing aircraft concept, an approach using ASTROS for structural and aeroelastic analysis was also undertaken to further refine these predictions. A simplified presentation of these finite element models, showing the skin panels only, appears in Figure 3. Here, a planar wing (no vertical separation between the leading and trailing wing roots) and a non-planar wing are presented. The fuselage mass and moment of inertia are modeled via a constraint element.
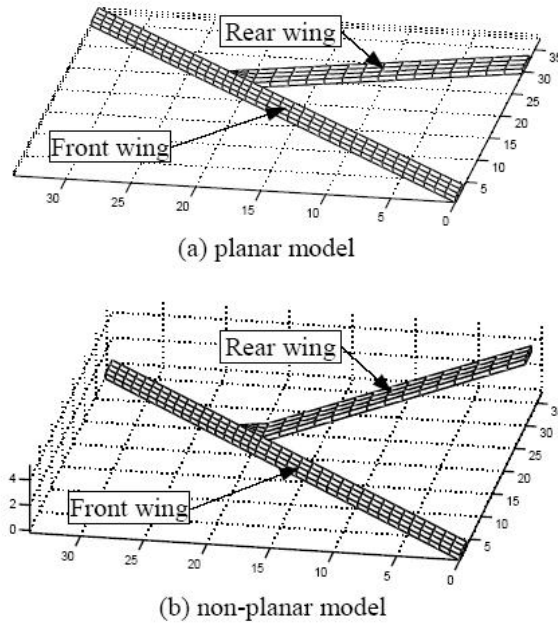

(a) planar model

(b) non-planar model

Figure 3 Finite element models of joined wings (only skin elements in these views).

The improved fidelity modeling of ASTROS provided a prediction of the transition from body-freedom flutter to cantilever flutter. This additional fidelity also allowed an investigation of how the aircraft's center of gravity affects the flutter modes. In Figure 4 below, results for a leading-wing sweep of 45° appear. A trend for transition similar to that predicted by the Ritz approach appears in this plot. The 10-ft position of the aircraft's center of gravity is the fore most position; the 15-ft position, the location

3

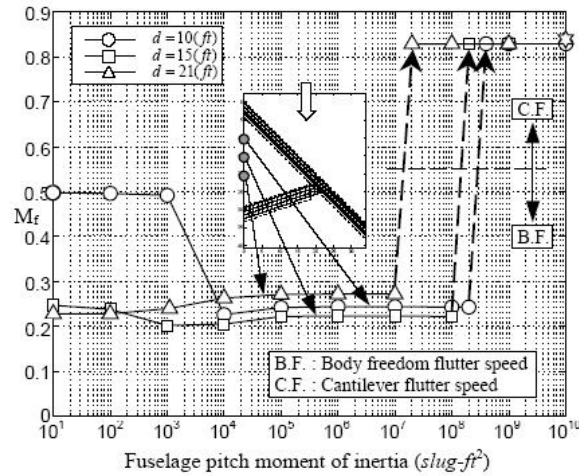with a minimum body-freedom flutter speed; the 21-ft location, the aft most position to avoid pitch instability.

Figure 4 ASTROS predicted body-freedom to cantilever flutter transition for 45° leading wing sweep.

As a result of this work, an important feature of the joined-wing configuration was highlighted; this feature is body-freedom flutter involving frequency interaction of the first elastic wing mode and the aircraft short period mode. In most of the parametric studies, the body-freedom flutter speed was less than the wing cantilever flutter speed, which is independent of the fuselage inertia. As the fuselage pitching moment of inertia was increased, the body-freedom flutter speed increased. When the pitching moment of inertia reaches a critical value, transition from body-freedom flutter to cantilever flutter occurred.

The effects of composite laminate orientation on the front and rear wings of a joined-wing configuration were also studied. An aircraft pitch divergence mode, which occurred because of the forward movement of the wing's center of pressure as it deforms under load, was discovered. Both body-freedom flutter and cantilever-like flutter were predicted depending upon the combination of front-wing and rear-wing ply orientations.

The optimization features of ASTROS allowed weight minimization of joined-wing designs, using planar and non-planar planforms with both isotropic (metals) and composite materials. Because body-freedom flutter was identified as a significant concern, these optimization runs were conducted using stress, displacement and body-freedom flutter constraints. A representative solution for a non-planar wing optimization, using metallic materials, appears in Figure 5. As typical of most of these studies, the wings increase skin thickness near the roots of both wings; outboard of the joint, the skin thickness approached the minimum gage limit. The optimized joined-wings using composite materials had lower weights than those of the metallic wings.
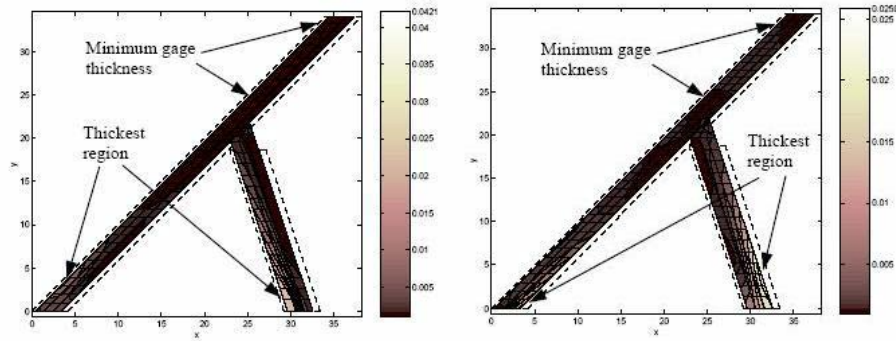
4

Figure 5 Upper surface (left) and lower surface (right) skin thickness distribution for a non-planar joined wing optimization using stress, displacement and body-freedom flutter constraints.

Joined-wing flutter characteristics are also impacted by the fuselage flexibility. Both the predicted elastic mode shapes of the wing and the flutter speeds are affected by fuselage deformation. As the fuselage flexibility increases, the body-freedom flutter speeds decrease. Related to this, the optimum weight of a joined wing increases as fuselage flexibility increases.

A box-wing configuration provided a final joined-wing configuration example. Aeroelastic analyses of the box wing investigated the effects of the center of gravity location and the pitching moment of inertia on the aircraft's flutter speed.

DOCUMENTATION

Portions of this work also appeared in a conference paper, and full documentation appears in one PhD thesis.

Lee, D. H., "Aeroelastic Tailoring and Structural Optimization of Joined-Wing Configurations", Ph.D. Thesis, School of Aeronautics and Astronautics, Purdue University, West Lafayette, IN, Aug. 2002.

T. A. Weisshaar and D. H. Lee, "Aeroelastic Tailoring of Joined-Wing Configurations", AIAA-2002-1207, Apr. 2002.

WING DESIGN WITH INTEGRATED ADAPTIVE CONTROL SURFACES

The goal of aeroservoelastic design is to find a lightweight wing with low control costs and high aerodynamic performance; these goals hold for the design of a wing with integrated adaptive control surfaces. This topic area investigated the design of wings with conformal control surfaces, inspired by the devices demonstrated by the DARPA Smart Wing program.[1] The nature of adaptive structures, like those that could be employed to provide flight control without using traditional hinged-control surfaces with gaps, requires that attention be given to control effectiveness. Some advanced controllers have limited ability to create forces and moments. As a result, the host structure must be designed to interact favorably with the available input.

A computational wing model was developed for these studies. The baseline wing model has a planform area of 175 ft^2, an aspect ratio of 3.2, a leading edge sweep angle of 45°, and a taper ratio of 0.2. The material is aluminum, with 11 spars. The trim case is at high q, sea level, V = 750 ft/s, with a supported load of 5,000 lb. A single set of symmetric wing loads is considered in this study.

Using ASTROS, the structural elements of this design were optimized for minimum wing weight. For this wing, the wing weight and associated aspect ratio were predicted. The baseline analysis has a stress constraint, a flutter constraint, and a 0.30 ft maximum tip displacement constraint. The optimized wing weight is 122 lb and the induced drag is 90 lb. The stress results indicate that the loads used only a few of the spars and only the a few ribs are sized beyond minimum gauge. In a design process, these results would lead to removal of some spars for the next level design. Figure 6 presents the upper wing skin thicknesses for this optimized design.
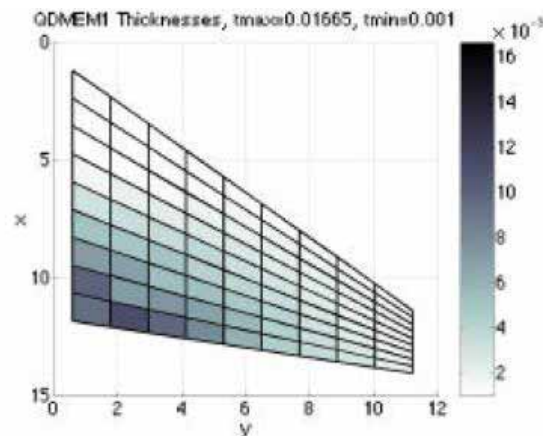

Figure 6 Upper skin thickness distribution for weight-optimized, baseline planform wing.

Starting from this baseline wing model, predictions of the work done by a conformal control surface was investigated. When a control surface is deflected, the pressure distribution over the wing changes, and the surface does work against these pressures. Since the distance that surfaces move determines the work done, aeroelasticity is important. To illustrate the use of control energy information, our example planform was used, but with a full-span 1° deflected control surface (flap-to-chord ratio 0.2) added to generate extra lift. To accommodate this lift, the aircraft weight was increased from 5000 lb to 10,000 lb; this approach mimics a symmetric, 2-g pull up loading condition. Only strength constraints are used during the weight minimization. The study was done to determine the effects of sweep and aspect ratio on energy required to deflect the flap. The airspeed was set at 750 *ft/s*. Figure 7 shows how the control surface energy distribution changes with sweep angle. The plot on the left demonstrates a swept-wing planform, the plot on the right demonstrates an unswept planform with the same aspect ratio, taper ratio and area.
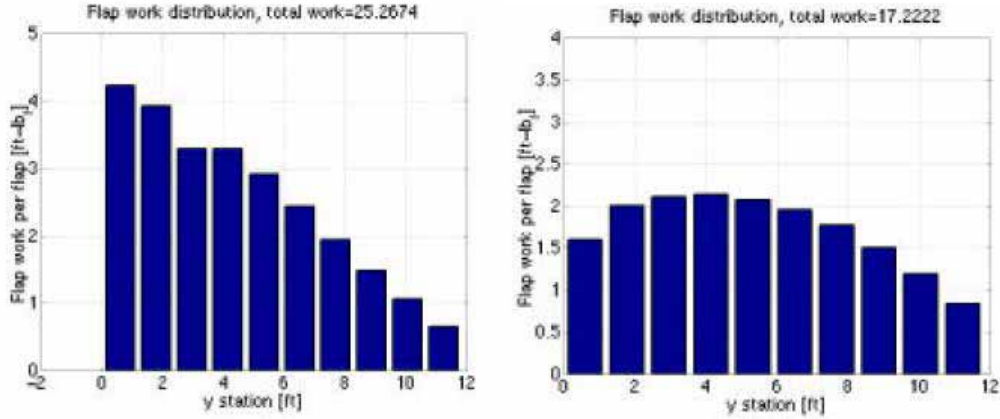
Figure 7 Control surface energy (work) distribution for conformal control surface on a swept (Λ = 45°) wing (left) and an unswept (Λ = 0°) wing (right).

The distribution of control actuator energy is different in the two cases, indicating that aeroelastic effects and aerodynamic effects have a marked effect on the work done by this surface. The ability to generate this type of information is required for an integrated design effort, in order to balance weight, aerodynamic performance (induced drag), and control surface work in an appropriate manner.

A parametric trade study was performed to determine the response surfaces of the weight, induced drag, and control work expended for varying aspect ratio and sweep. Five sweep angles (45°, 35°, 30°, 15°, and 0°) and four aspect ratios (2.5, 3.2, 4.2, and 5.2) were used. The wing area, thickness, and taper ratio were kept at the same value as the baseline wing described above. The weight of each wing was minimized subject to strength constraints under the single aerodynamic load condition described above. To simplify this portion of the investigation, flutter and tip displacement constraints were not included.

Figure 8 shows the effects of sweep and aspect ratio on optimized weight. It can be seen that for low aspect ratio wings, sweep angle does not greatly affect weight, although at higher aspect ratios flexibility becomes more important. Lower aspect ratio is generally better to reduce weight.
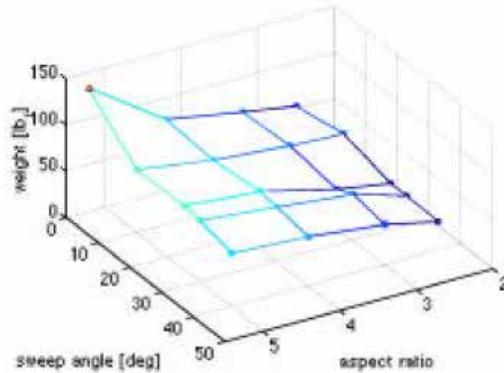

Figure 8 Optimized wing weights as a function of sweep and aspect ratio.

Figure 9 shows the effects of sweep and aspect ratio on induced drag. Here, it can be seen that wing sweep, except at high aspect ratios, does little to affect the induced drag (it does affect wave drag however), but aspect ratio has a large effect.
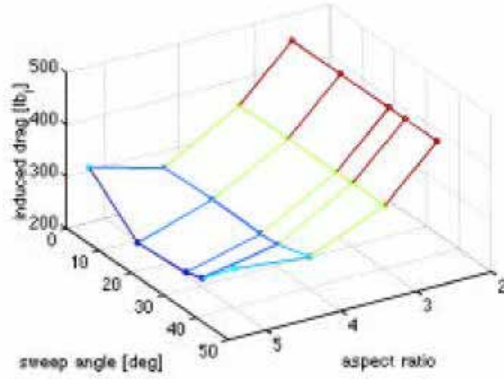
7

Figure 9 Induced drag as a function of sweep and aspect ratio for weight-optimized wings.

Figures 10 and 11 show the effects of sweep and aspect ratio on the control energy and on the flap effectiveness, respectively. Generally, high aspect ratio is favorable for low control energy, confirming the previous results, though the magnitude of this effect depends on sweep angle. The flap effectiveness, defined here as the derivative of the lift coefficient with respect to flap angle, has trends nearly opposite that of the control energy trends. This is reasonable since the less effective the flaps are, the more work required to deflect them.
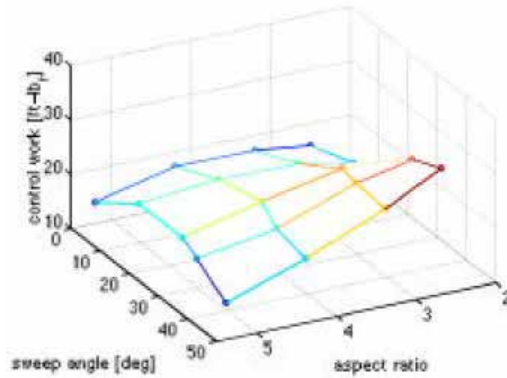

Figure 10 Total control work as a function of sweep and aspect ratio for weight-optimized wings.
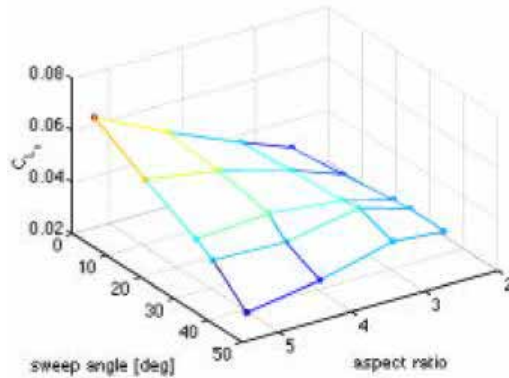

Figure 11 Flap effectiveness ($(C_L)_\delta$) of weight-optimized wings as a function of sweep and aspect ratio for weight-optimized wings.

This study demonstrated the types of calculations needed to for design and aeroelastic optimization of aircraft lifting surfaces with conformal control surfaces. This method indicates that the configuration or planform variations result in different structurally optimized designs, in terms of total wing weight, induced drag and control surface energy. The approach and corresponding calculations produced results consistent

with existing design space experience and provided information useful for extending this experience to a non-traditional wing control concept.

DOCUMENTATION

The full scope of this effort is documented in one conference paper and one MS thesis.

Henderson, J. A., Weisshaar, T. A., and Sanders, B., "Integrated Wing Design with Adaptive Control Surfaces", AIAA 2001-1428, Apr. 2001.

Henderson, J. A., "Formal Design Space Evaluation and Optimization for Innovative Aeroelastic Concepts," M.S. Thesis, School of Aeronautics and Astronautics, Purdue University, West Lafayette, IN, May 2001.

---

[1] J. Kudva, K. Appa, A.P. Jardine, C. A. Martin and B.F. Carpenter, "Overview of Recent Progress on the DARPA/USAF Wright Laboratory Smart Materials and Structures Development-Smart Wing Program," Proceedings of the SPIE Smart Structures and Materials Conference 1997: Industrial and Commercial Applications of Smart Structures Technologies, edited by J.M. Sater, Vol. 3044, International Society for Optical Engineering, Bellingham, Washington, 1997, pp. 24-32.

AEROELASTIC DESIGN AND ANALYSES OF MORPHING WINGS

The investigations in this topic area involved studies of two morphing wing configurations, a telescoping wing and an out-of-plane folding wing. These two concepts would allow significant changes in wing area and aspect ratio during flight. Because these concepts are rather different than current fixed geometry, or even variable sweep wings, the investigations sought to determine how allowing the significant changes in wing planform geometry might affect aeroelastic response, such as flutter speed, and might impact the weight of the wing.

TELESCOPING WING

The telescoping wing investigations relied upon ASTROS as the analysis tool. A telescoping wing concept was modeled for use within ASTROS. The structural features of the telescoping wing were modeled using CQUAD4 elements for the wing skin. For the inboard portion of the wing, the structural skin extended from 0.1 x/c to 0.7 x/c to allow space for leading and trailing edge devices. The structural skin extended over the entire chord of the outboard (telescoping) section. Figure 12 presents this model.
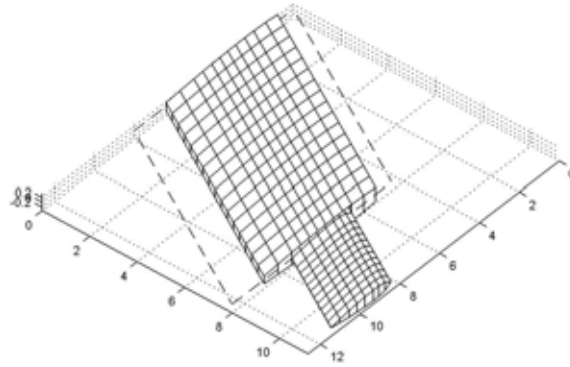

Figure 12 Structural skin model for telescoping wing.

An actual telescoping wing would incorporate structure and mechanisms to allow the outboard section to extend and retract while in flight. For the aeroelastic investigations, the structural portions of this were modeled as rails using CBAR beam elements. The ribs and spars of both wing sections were modeled with shear elements, as displayed in Figure 13.
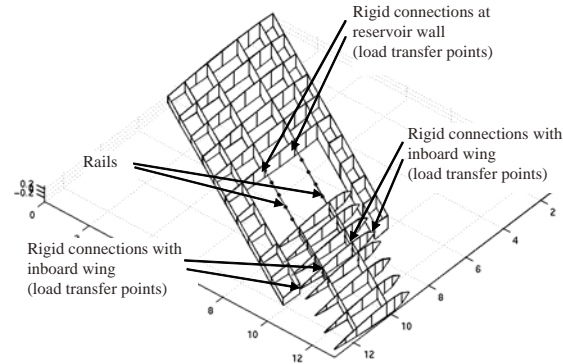
Figure 13 Internal wing structure model for telescoping wing.

The aerodynamic modeling of the telescoping wing maintained a 30° sweep for the wing. For these studies, the inboard wing section is modeled with a NACA 0009 airfoil section and the outboard section is modeled with a NACA 0015 section. This allows the inboard and outboard wing to have matching absolute thickness. This is not a requirement for the telescoping wing model, rather it is a convention used for this study. Figure 14 shows the aerodynamic modeling approach. For the panel aerodynamics, the

10

intersection between the inboard and outboard wing sections required a compromise approach in order to generate a load distribution across the wing with the outboard section extended.
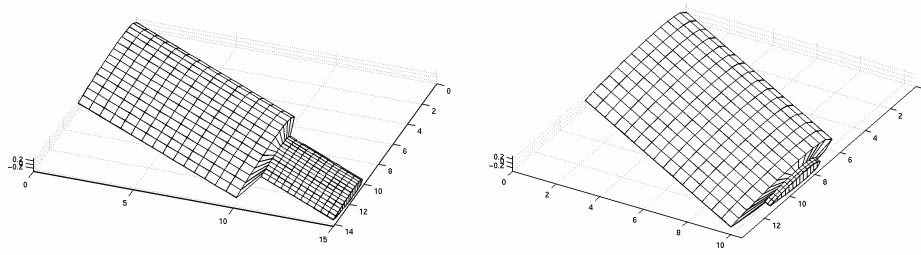

**Figure 14 Aerodynamic panels on telescoping wing
with 100% extension (right) and 10% extension (left).**

A weight minimization problem was then developed for the telescoping wing. In this study, the wing skin, spar, rib and rail thicknesses were used as design variables. ASTROS provided both the optimization algorithm and the flexible wing (aeroelastic) analysis. Both a 1-g cruise and 6-g maneuver condition were investigated, but the wing optimization was conducted for only one condition at a time with one planform (i.e. an optimal wing was found for the 1-g cruise with the outboard wing 100% extended, and another optimal wing was found for the 6-g maneuver with the outboard wing only 10% extended). This was done because the standard modeling approach within ASTROS does not allow for change of the structural geometry of the wing within one optimization / analysis run. As part of the study, the chordwise position of the outboard wing section relative to the inboard section was changed among the most forward possible position, the mid-chord position, and the aft-most position.

For comparison, a "non-morphing" wing with the same planform as the extended telescoping wing were also examined using a weight minimization approach. The non-morphing planform did not contain the rail elements or the reservoir box area, but did use the skin, spar and rib thicknesses as design variables. As with the morphing wing, one non-morphing wing was optimized for the 1-g cruise condition, and one was optimized for the 6-g maneuver.

The results of these optimization studies led to several observations. In the 1-g cruise condition, the morphing wing design had weights between 217% and 250% of the non-morphing wing weight. This might be expected because the morphing wing required design of the rails to transfer loads from the outboard section into the inboard section. As the location of the outboard section moved aft, the difference in weight increased, suggesting that having the quarter-chord positions of the two wing sections misaligned results in an increase in weight.

For the 6-g maneuver, the optimum morphing wing weight was between 87% and 99% of the non-morphing wing weight. The largest difference occurred for the aft-most position of the outboard section, so that the lightest morphing wing had the rails and reservoir further aft in the wing, where the externally applied pressure loads are lower. This suggests that a morphing wing may actually have a lower empty weight if designed to be retracted during high maneuver load conditions.

The weight of the rail, reservoir and stringer elements modeling the morphing components of the wing appear to be insensitive to the chordwise position of the outboard wing section. For all three locations, the weight of this "morphing structure" maintained essentially the same percentage of empty weight for both the 1-g and 6-g load conditions.

FOLDING WING

Studies of an out-of-plane folding concept were also conducted as part of this topic area. These studies focused upon flutter prediction, rather than structural optimization. For this effort, the wing model was developed with dimensions appropriate for a medium sized UAV, with a wing span of 31 feet. Figure 15 presents the starboard wing planform along with relevant dimensions. The overall leading edge sweep of

the wing is 45°. The wing can fold out-of-plane along the root chord and along the chord located 5.5 feet from the root; this folding reduces the wing's span and planform area.
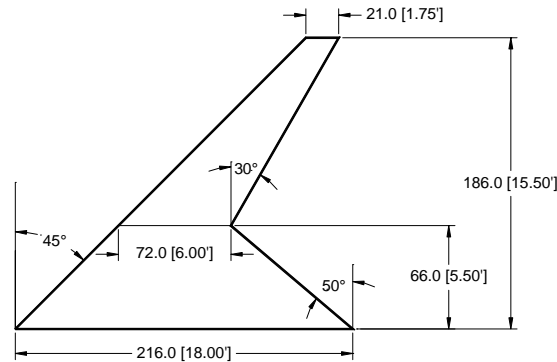

Figure 15 Folding wing planform (starboard only).

The basic structural skin, rib and spar models were constructed for the folding wing as they were constructed for the telescoping wing. The significant modeling difference for the folding wing is the hinges used at the fold lines; these hinges are modeled using rigid steel bars. Connections between the wing hinges and the wing structure utilize virtual nodes. Figure 16 presents a view of the wing model looking forward from behind the wing.
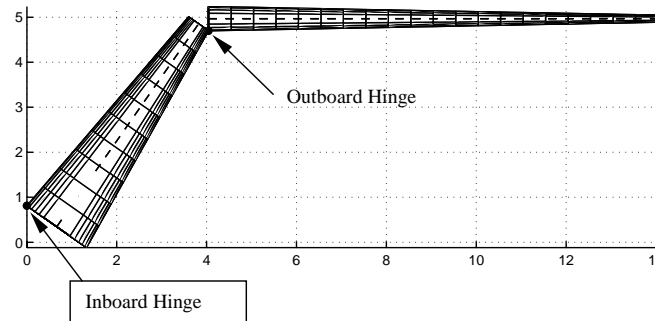

Figure 16 Wing model illustrating hinge locations and rotations.

With this out-of-plane folding wing model, the hinge actuation is governed by the rotation of the inboard hinge; the outboard section of the wing remains parallel to the "ground". No structural optimization was performed. Only the flutter speed characteristics of this wing were investigated at inboard hinge angles between 0° (wing fully extended) and 90°. The outboard hinge was kept constant during these investigations, but the inboard hinge bar was varied in cross-sectional diameter, which increases the stiffness of the hinge.

As might be expected, the larger inboard hinge diameter results in a heavier wing weight. The larger hinge diameter also has a higher flutter speed at 0° hinge angle, which is anticipated from the increased stiffness. The increase in weight varies like d^2, as is expected, while the increase in flutter speed appears to follow a trend like $d^{1/2}$ or $d^{1/3}$. This trend is displayed in Figure 17.

At different inboard hinge angles, the highest flutter speed is not always associated with the largest inboard hinge diameter. For two combinations of inboard and outboard hinge diameter, the flutter Mach number was computed for various hinge angles. Figure 18 presents this variation. It appears important to consider intermediate positions as part of any out-of-plane morphing wing design problem that considers flutter.
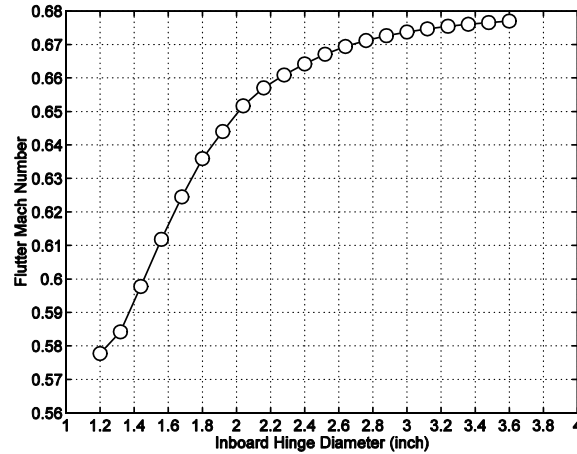
Figure 17 Flutter Mach number vs. inboard hinge diameter (hinge at 0°).
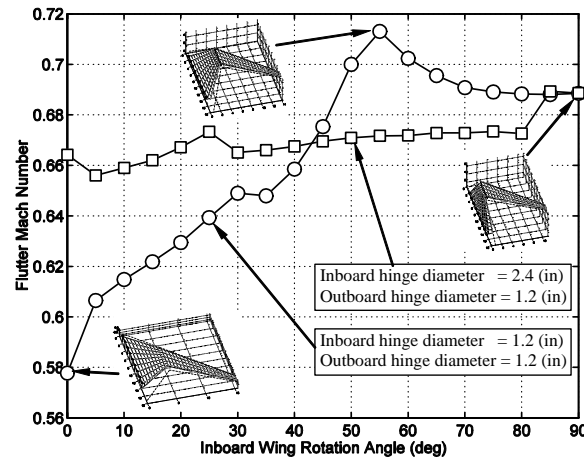

Figure 18 Flutter Mach number vs. inboard hinge rotation angle for two combinations of inboard and outboard hinge diameter.

Because structural optimization was not conducted on this configuration, the rib, spar and skin thicknesses remained constant throughout the study. The purpose of this study was to investigate flutter speeds, but with the initially chosen structural thickness, flutter was not predicted for the wing. By increasing the spar and rib thicknesses on the outboard wing, flutter could be generated. Obviously, the altered mass distribution affects the flutter prediction, but it should not be concluded that this folding wing concept is "flutter free".

DOCUMENTATION

This work is documented in two reports:

Lee D. H., "Telescoping Morphing Wing Weight Optimization with Static Aeroelastic Constraints", School of Aeronautics and Astronautics, Purdue University, West Lafayette, IN, Dec. 2002.

Lee D. H., "Folding Wing Flutter Analysis Results" School of Aeronautics and Astronautics, Purdue University, West Lafayette, IN, May 2003.

ENERGY AS AN OBJECTIVE FOR SHAPE OPTIMIZATION OF MORPHING AIRFOILS / WINGS

Recent advances in materials science and actuation technologies have led to interest in morphing aircraft[2]. The wings of a morphing aircraft might use smooth, deformable leading and trailing edges, or even possibly fully deformable airfoil sections instead of conventional, discrete movable control surfaces. The concept of a morphing aircraft has generated a new design aspect that must be addressed in aerodynamic configuration design and optimization. Generally, a multi-point problem formulation is used for airfoil or wing design. A weighted sum of drag coefficients, computed at various design flight conditions, serves as an objective, and constraints ensure that the lift coefficient matches specified values at each of the flight conditions. The resulting shape has performance that is essentially a compromise over the flight conditions. In the case of a morphing aircraft, the wing would be able to change its shape during flight. It should be possible to adjust the wing shape to the best possible shape for any flight conditioned encountered by the aircraft; this would suggest that the morphing airfoil could be designed using a series of single-point problem formulations. However, there is an actuator effort "cost" associated with these shape changes. Thus the effort required to affect the morphing must be included in the optimization process.

The research here focuses upon the shape design of morphing airfoil sections. In the efforts to be described, the relative strain energy needed to change from one airfoil shape to another is presented as a design objective for minimization, while constraints are enforced on the lift and drag coefficients. A newly found airfoil set with small relative strain energy requires small actuation cost and increases the benefits from multi-mission capability.

SCOPE AND METHODS OF APPROACH

To conduct the investigations of energy as an objective in the morphing airfoil shape optimization problem, two parallel efforts are underway. The first uses a very simplified aerodynamic analysis to investigate problem formulation and solution strategies, while the second uses higher fidelity aerodynamic analyses to provide more accurate predictions. However, both approaches are used to highlight how strain energy can be included as a measure of actuation effort. In effect, there exists a trade-off between the morphing energy and the aerodynamic performance.

REPRESENTATIVE PROBLEM

Some recent studies by the US Air Force Research Laboratory (AFRL) have focused upon a high-altitude, long-endurance aircraft platform. A notional representation of this concept appears in Figure 19. This aircraft's design mission includes a 40+ hour loiter segment, during which the aircraft will experience a significant weight reduction as it consumes most of its fuel. If the aircraft is intended to loiter at a constant altitude and constant airspeed, a fixed geometry wing would not be operating at its most efficient conditions throughout the mission. However, if the aircraft utilized a wing with morphing airfoil sections, it would be possible to change airfoil shape throughout the mission in order to improve the endurance performance of the aircraft.
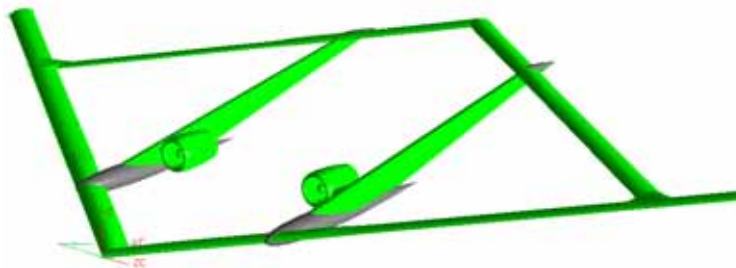

Figure 19 Notional high-altitude, long endurance aircraft concept.

Based upon systems studies from AFRL, the required lift coefficients are known at various times during the long loiter segment. To begin the energy objective investigations, the flight conditions at three points in time provide the airfoil shape design conditions. These are summarized in Table 1. Near the start of the loiter segment, the aircraft's weight is high, and the required design lift coefficient is also high. Because of the desire for constant altitude, constant velocity loiter, the Reynolds number and Mach number for all three conditions are the same. The low Mach numbers should not require aerodynamic analyses that include wave drag.

Table 1 Airfoil design conditions.

	Condition 1	Condition 2	Condition 3
Design lift coefficient	1.52	1.18	0.85
Mach number	0.6	0.6	0.6
Reynolds number	1.5×10^6	1.5×10^6	1.5×10^6

LOW-FIDELITY AERODYNAMICS APPROACH

The low-fidelity aerodynamic analysis approach was undertaken because the time required for analyses is very short, allowing relatively rapid optimization studies. The aerodynamic analyses used in this approach are based upon the extended Joukowski airfoil conformal mapping approach presented by Jones[3] to compute pressure distributions and upon the approach presented by Houghton[4] to compute the viscous boundary layer. For the conformal mapping approach, the Joukowski airfoils are described by five variables: x_c, y_c, x_t, y_t, and δ.

INCREASED FIDELITY AERODYNAMICS APPROACH

For additional accuracy the well-known XFOIL[5] code is selected as a function evaluator. XFOIL is suitable for low Reynolds number airfoil flows with transitional separation bubbles. A linear-vorticity panel method with a Karman-Tsien compressibility correction is used for inviscid calculation. While this is not generally considered a high-fidelity analysis tool, it does provide greater resolution of the airfoil shape and incorporates more advanced approaches for prediction of viscous effects.

To pose the airfoil shape optimization problem when using XFOIL, the design variables that control the airfoil shape are needed. In the approach used for this paper, Hicks-Henne shape functions[6,7] are added to a baseline airfoil shape. The design variables are multipliers that determine the magnitude of the shape function as it is added to the baseline shape. The y-coordinate positions of the upper and lower surface of the airfoil are then described as functions of the x-coordinate position using the following equation:

$$y(x) = y(x)_{\text{Base Airfoil}} + \sum \xi_i f_i(x) \tag{1}$$

where ξ_i are the design variables; and f_i, the shape functions ($i = 1, 16$ here).

Figure 20 depicts the shape functions and shows their individual effects on a baseline NACA 0012 airfoil along with the upper and lower limits of the airfoil surfaces. The upper limits, shown in red, are reached when all design variables ξ_i are at their upper bounds; similarly, the lower limits, shown in blue, are reached when ξ_i are all at their lower bounds.
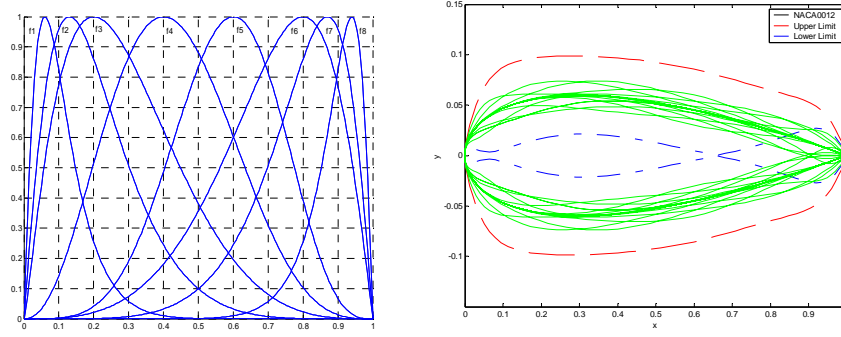
Figure 20 Hicks-Henne shape functions (left) and shape functions applied to a NACA 0012 base airfoil (right).

STRAIN ENERGY AS AN OBJECTIVE

As mentioned previously, a morphing airfoil could theoretically provide aerodynamically optimal shapes at any flight condition. However, morphing requires extra mechanisms to effect shape changes. This work uses the assumption that the energy needed to change the airfoil shape is proportional to the actuation system weight. The purpose of this research is to reduce the extra system weight of morphing devices needed to acquire aerodynamic performance benefits. The objective function, then, is to minimize the strain energy for changing the shape of the airfoil.

However, there are several ways to model the strain energy needed to change the airfoil shape. All of these ways make use of the basic idea that the strain energy in a structure is proportional to the square of the change in length of the structure. In this paper, two simple strain energy models have been employed. The first is described by equation (2) using the internal linear spring model concept suggested by Prock, et al[8].

$$U = \sum_{i=1}^{n} \frac{1}{2} k_i \Delta L_i^{\,2} = \sum_{i=1}^{n} \frac{1}{2} \frac{EA}{L_i} \Delta L_i^{\,2} \tag{2}$$

In this equation, U is the strain energy; k_i, the spring constant, EA the spring axial stiffness, and ΔL_i the spring deformation. With no real actuation system envisioned as yet, the spring model strain energy objective does not need to include the EA terms.

This model assumes that springs connect the upper and lower airfoil surfaces; as the airfoil morphs, the springs deform, which corresponds to an amount of strain energy. Figure 21 presents a simple illustration of this model.
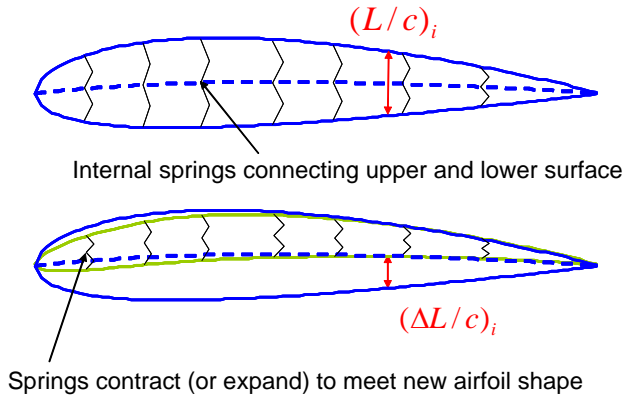

$(L/c)_i$

Internal springs connecting upper and lower surface

$(\Delta L/c)_i$

Springs contract (or expand) to meet new airfoil shape

Figure 21 Internal linear spring model for strain energy.

The second model used in this study measures deformation of the airfoil surface. The total circumference of the airfoil changes as the airfoil morphs to assume different aerodynamic shapes. Using the change in circumference squared can also provide a measure of strain energy needed for morphing. Like the linear spring model, this approach does not yet include a mechanism or actuation scheme to provide the shape changes, but would be much like the effect of inflating or deflating a balloon. Figure 22 illustrates this concept; here, the relative strain energy would be proportional to $(s_1-s_2)^2$.
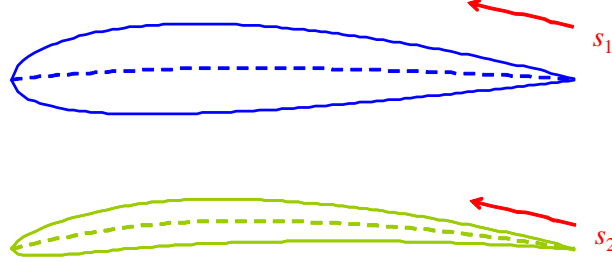

Figure 22 Airfoil circumference or "balloon effect" model for strain energy.

To formulate the objective function, relative strain energy terms, U_{ij}, representing the strain energy associated with changing from shape i to shape j. Currently, the objective incorporating strain energy is to minimize the maximum relative strain energy value associated with the shape changes. For the three conditions used here, the objective appears as:

$$\text{Minimize } [\text{Max}(U_{12}, U_{23}, U_{13})] \tag{3}$$

In addition, three different inequality constraints on the drag coefficient and equality constraints on the lift coefficient were applied. The reference drag coefficients were selected as minimum drag value from the single objective optimization results of each constrained flight condition.

Subject to,

$$C_l = C_{l_1}, \quad C_{d_1} \leq C_{d_{1_0}}$$
$$C_l = C_{l_2}, \quad C_{d_2} \leq C_{d_{2_0}}$$
$$C_l = C_{l_3}, \quad C_{d_3} \leq C_{d_{3_0}}$$

These current strain energy models do not directly account for an actuation or mechanization strategy to change the airfoil shapes. It is anticipated that results using the two models might suggest different amounts of energy needed to obtain desired aerodynamic performance. If this is the case, the results would suggest that different, realizable actuation strategies would also require different amounts of energy. As physically realizable actuation strategies become available, these models can be used to also assess strain energy or actuation energy in the same optimization framework as the two simple models presented above.

OPTIMIZATION ALGORITHM

Since its first descriptions, the Genetic Algorithm (GA) has been applied to many engineering optimization problems. A GA has the ability to search highly multimodal, discontinuous design spaces and also locates designs at, or near, the global optimum without requiring a good initial design point. Because the nature of the min-max objective formulation may have discontinuous derivatives and because airfoil shape design problems appear to frequently have local minima, the GA provides a search method that would not be hindered by these issues.

Commonly, using a GA for design optimization is computationally expensive. For the low-fidelity conformal mapping approach for aerodynamic analysis, the run time of the GA is not prohibitive, so a serial genetic algorithm has been used. However, the XFOIL aerodynamic analysis requires more computational effort, and a serial implementation of the GA would result in prohibitive run times. To overcome the computational time problem, parallelization of the GA is needed. In this research, a Master-Slave type parallelization is applied to convert a serial GA into a parallel program, and a Linux-Cluster machine is used for calculation following the approach of Ref. 9. As a relatively small communication

17

time is needed for the parallel GA, the code scales well on the 52-Processor Linux Cluster used for the runs.

INVESTIGATION AND RESULTS

Currently, both the low-fidelity and higher-fidelity approaches have been used to generate airfoils using single-point problem formulations that correspond to each of the flight conditions given in Table 1. These are intended to represent the best possible aerodynamic shapes for the airfoils, but these shapes were generated without concern for the energy needed to change from one shape to another. In Figure 23, the resulting airfoils from the three single-point optimization runs are superimposed on each other to demonstrate the type of shape changes that would be required for morphing the airfoil to meet the three flight conditions.
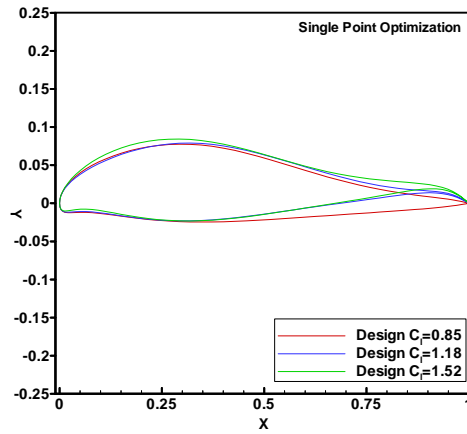
Figure 23 Airfoil shapes from single-point optimizations using XFOIL analyses.

Also, both approaches can generate airfoils using a multi-point problem formulation to find a single fixed-geometry shape that compromises between all three flight conditions. This is the traditional approach for airfoil design, and this resulting shape is associated with zero strain energy, because this assumes the airfoil maintains a constant shape for all flight conditions. Figure 24 shows this resulting compromise shape from the multi-point problem formulation.

Figure 24 Airfoil shape from multi-point optimization using XFOIL analyses.

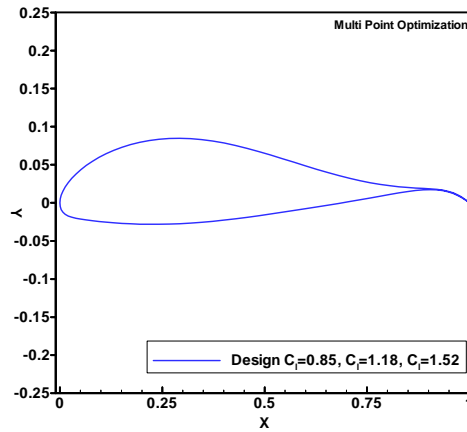Between these two extremes – the best set of aerodynamic shapes that would require a significant amount of energy to change between and the best compromise single shape that requires no energy – a tradeoff exists between the energy needed to change between shapes via morphing and the aerodynamic performance increase available from the shape change. To generate these tradeoff shapes, an epsilon-constraint formulation converts the two-objective problem into a single objective problem in which one objective becomes the primary objective, and the other objective is handled using a constraint. By varying the limiting value in this constraint for each optimization, several Pareto optimal points are obtained that illustrate the tradeoff between the aerodynamic objective and the strain energy objective. Figure 25 presents the tradeoff obtained using this approach. The green triangle in this plot represents the multi-point airfoil shape associated with zero energy, but having the highest sum of the three drag coefficients. The blue square represents the set of three shapes found from three single-point shape optimizations; this set has the best aerodynamic objective performance, but the highest energy objective. The red diamonds represent sets of three airfoil shapes generated using the epsilon-constraint approach to find tradeoffs between the aerodynamic performance and the energy requirements.
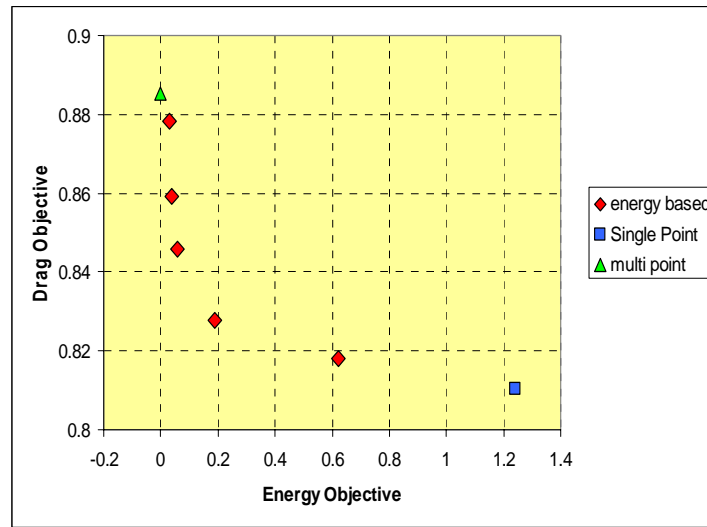
Figure 25 Pareto front of optimal tradeoffs between drag and energy for morphing airfoils.

The set of airfoil shapes located at the "knee" in the tradeoff curve (with an energy objective of 0.1897 and a drag objective of 0.8277) appears in Figure 26. At this knee in the curve, there is a significant improvement in aerodynamic performance with a limited increase in the energy requirements for shape change. As evident in the figure, the three shapes are very similar to keep the strain energy low, but making large enough changes to improve the drag coefficient at each flight condition.

Figure 26 Morphing airfoil shapes at "knee" of tradeoff between the drag and energy objectives.

Additional efforts in this topic area would be welcome. These should include a more comprehensive study of the multiobjective problem formulation, the use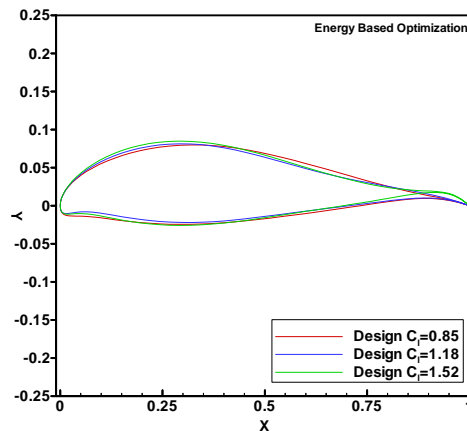 of higher-fidelity solvers, application to problems in which the morphing airfoil experiences flow at several different Mach numbers (even "tri-sonic" problems where the airfoil must perform at subsonic, transonic and supersonic conditions), and incorporation of actuation schemes with predictable energy requirements.

DOCUMENTATION

The full scope of this effort is documented in two conference papers and one MS thesis. Additionally, one PhD thesis and one MS thesis are in progress based upon this effort. The most recent efforts in this topic area will be presented at the 43rd AIAA Aerospace Sciences Meeting in January 2005.

Prock, B. C., "Energy Based Design for Morphing Aircraft Wings", M.S. Thesis, School of Aeronautics and Astronautics, Purdue University, West Lafayette, IN, Aug. 2002.

Prock, B. C., Weisshaar, T. A., and Crossley, W. A., "Energy as an Objective for Airfoil Shape Change Optimization," AIAA-2002-5401, Sep. 2002.

Namgoong, H., Crossley, W. A., and Lyrintzis, A. S., "Issues for Global Optimization in Multipoint Transonic Airfoil Design," AIAA-2002-5641, Sep. 2002.

Namgoong, H., Nankani, K., Crossley, W., and Lyrintzis, A., "Using Energy as an Objective for Morphing Airfoil Shape Optimization," to be presented at 43rd AIAA Aerospace Sciences Meeting, Reno, NV, Jan. 2005.

Nankani, K., "Optimization Approaches for Morphing Airfoils using Drag and Strain Energy as Objectives," M.S. Thesis, School of Aeronautics and Astronautics, Purdue University, West Lafayette, IN, anticipated Dec. 2004.

Namgoong, H., "Airfoil Optimization for Morphing Aircraft," Ph.D. Thesis, School of Aeronautics and Astronautics, Purdue University, West Lafayette, IN, anticipated May 2005.

---

[2] McGowan, A.R. et al., "Recent Results from NASA's Morphing Project," SPIE Paper No.4698-11, 9th International Symposium on Smart Structure and Materials, 2002, SanDiego, California.

[3] Jones, R. T., *Wing Theory*, Princeton University Press, Princeton, NJ, 1990

[4] Houghton E.L., Carpenter P.W., *Aerodynamics for Engineering Students,* John Wiley & Sons, 1993

[5] Drela, M.,"XFOIL: An Analysis and Design System for Low Reynolds Number Airfoils," Conference on Low Reynolds Number Airfoil Aerodynamics, University of Notre Dame, June 1989.

[6] Hager, J. O., Eyi, S., Lee, K. D., "Two-point transonic airfoil design using optimization for improved off-design performance," AIAA Journal of Aircraft, Vol.31, No5, 1994, pp. 1143-1147.

[7] Hicks, R.M. and Henne, P.A., "Wing Design by Numerical Optimization," *Journal of Aircraft*, Vol.15,No.7, July 1978,pp.407-412.

[8] Prock, B. C., Weisshaar T. A., Crossley, W.A., "Morphing airfoil shape change optimization with minimum actuator energy as an objective", 9th AIAA/ISSMO Symposium on Multidisciplinary Analysis and Optimization, Atlanta, Georgia, 2002.

[9] Jones, B. R., Crossley, W. A., Lyrintzis, A. S., "Aerodynamic and Aeroacoustic Optimization of Airfoils via a Parallel Genetic Algorithm," *Journal of Aircraft,* Vol. 37, No. 5, Nov.-Dec. 2000, pp. 1088—1096.

MORPHING WING WEIGHT ESTIMATION USING OPTIMIZATION AND RESPONSE SURFACE METHODS

Morphing structures are of increasing interest for aerospace applications, particularly aircraft[1,2,3]. As these morphing concepts begin to further deviate from the "conventional" variable sweep wings and high-lift devices, new design techniques and optimization strategies must be simultaneously advanced to handle the increased variations of these systems from existing aircraft. Development of a fundamental set of design and optimization techniques at this level of complexity would allow for a more efficient technological advancement of these highly complex, adaptive systems.

One important issue for adaptable aircraft is that the benefit of the morphing technologies may not be evident at the subsystem or component level. Instead, the benefit of morphing may be apparent only at the aircraft system level. Currently, research is being done to optimally size types of morphing aircraft. However, these sizing codes are critically dependent on a prediction of the aircraft's empty weight. Since no prior experimental or empirical data exists for most of these morphing components, simple estimates based on conventional data are generally used to predict the morphing component's empty weight[4]. Although these estimates are usually based on seemingly reasonable assumptions, there is no guarantee that the prediction is accurate and any pertinent sizing results must be approached with some skepticism.

Clearly, if a credible weight equation could be developed for these morphing structures, further research in the overall sizing and optimization techniques of morphing aircraft would be more rigorously substantiated. The research presented here discusses the approach to deriving such an empirical equation. Acquisition of experimental data, response surface methodologies, and data regression techniques will be the key components in this investigation. At the time of submittal, a telescoping wing provides the morphing strategy for this investigation; other morphing strategies may also be investigated.

SCOPE AND METHODS OF APPROACH

The telescopic wing concept is currently used to illustrate the methods necessary to develop an empirical weight equation for a morphing structure. This type of wing consists of a fixed inboard section and an extendable outboard section. Figure 27 depicts the wing in its extended and retracted configurations, respectively.
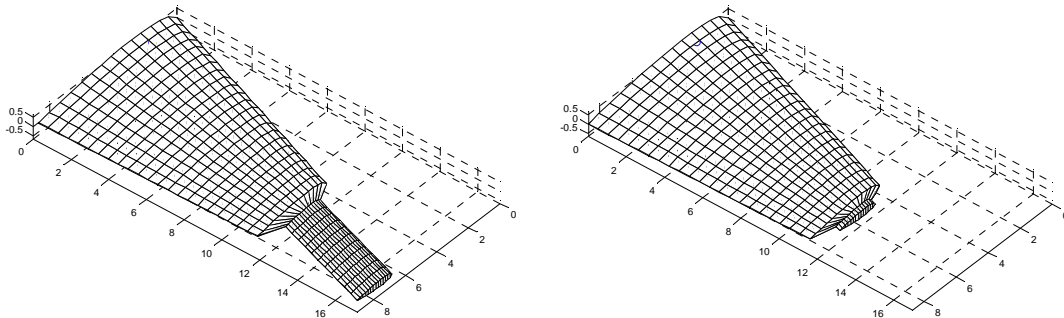

Figure 27 Telescoping wing in extended (left) and retracted (right) configurations.

A hollow shell (reservoir) will be required in the fixed portion of the wing to house the telescopic portion in its retracted configuration. Support for the outboard wing is currently modeled with two parallel I-beam rails separated chordwise. The rails not only provide structural reinforcement but also dictate the outboard wing's translational path. A similar layout and modeling strategy appears in the previous chapter, "Aeroelastic Design and Analyses of Morphing Wings".

This research relies on the optimized results of several finite element telescopic wing models. In this study, the software package ASTROS (Automated STRuctural Optimization System) was used to acquire all necessary data. The application of ASTROS to this research is extremely desirable because it is capable of coupling CFD, FEA, and optimization techniques into a single algorithm. During an optimization routine for example, the software is able to size the model's elements by considering, simultaneously,

various aerodynamic maneuver loads, flutter characteristics, and element constraints (buckling, Von Mises strength criterion, displacements, etc.).

OPTIMIZATION METHODOLOGY

Although ASTROS has an extremely versatile optimization algorithm, it is unable to account for both the extended and retracted geometries of the wing in a single run. Several techniques were investigated to alleviate these shortcomings but most were too costly to implement in this investigation. The current optimization scheme involves separate optimizations of the wing in both its extended and retracted configurations. Expected maneuver loads associated with the particular wing configuration (extended or retracted) are applied in their respective optimization runs. The resulting optimized models are then compared at an elemental level; the largest dimensions of each element are integrated into a final, pseudo-optimized model. Granted, if the resultant still satisfies all of the strength and aeroelastic constraints, the weight of this final model will be used as representative data in the response surface. Figure 28 provides a flow chart-like description of this two-model optimization process.
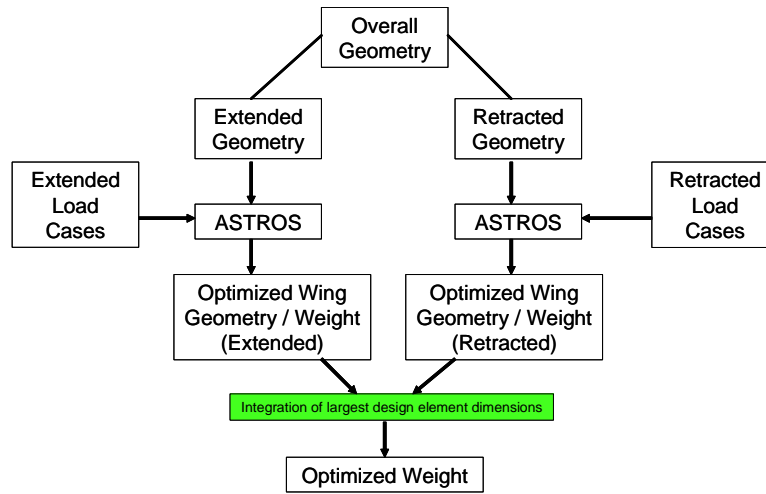

Figure 28 Two-model optimization process for morphing wing.

Figure 29 illustrates the integration process for the upper skin of the wing. Each panel's skin thickness is illustrated by the color of the panel: blue hues representing a thinner gage panel than the reddish hues. The two leftmost figures display the optimal skin thicknesses resulting from separate ASTROS runs. The final figure results from an integration of the previous runs as described above.
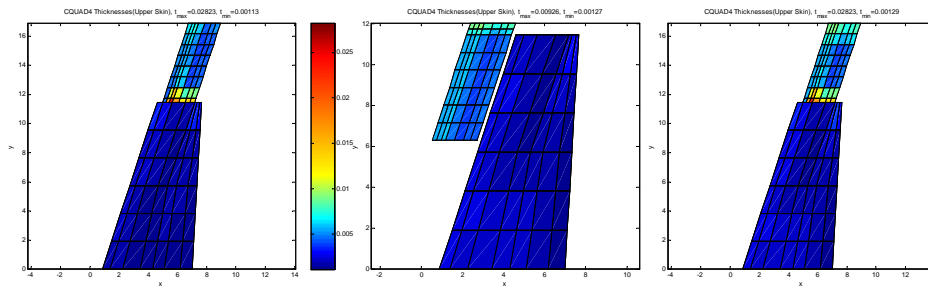
Figure 29 Upper skin thicknesses for extended configuration (left), retracted configuration (center), and aggregate design (right).

DEFINITION AND RANGE OF VARIABLES

A basic set of parameters was established to describe the overall geometry of the telescopic wing. This set contains variables which parallel those found in a conventional wing weight equation, yet also incorporates a variable to define the morphing capabilities of the wing. These parameters were bound such

that the domain of the overall design space would be representative of a small, unmanned, tactical bomber. The set of system variables and their associated bounds are summarized in Table 2.

Table 2 Morphing wing variables used to construct weight equations.

| Variable | Bounds | | Units | Description |
	Lower	Upper		
S	150	200	[ft^2]	Planform Area (Retracted)
AR	3.5	5	---	Aspect Ratio (Retracted)
λ	0.5	0.8	---	Taper Ratio (Retracted)
Λ$_{LE}$	20	40	[deg]	Leading Edge Sweep (Retracted)
t/c	9	15	[%]	Thickness to Chord Ratio
W/S	60	100	[lb/ft^2]	Wing Loading (Retracted)
Δb/b	0.5	0.75	---	Maximum Change in span / Retracted span

EXPERIMENTAL DESIGN

A large number of data points would be required to produce an equation that is relatively accurate over the entire region of the design space. The cost of obtaining a single data point as previously described is computationally expensive (on the order of 2-3 hours), therefore, finding a minimum set of data points that provides adequate coverage of the response surface is strongly desired.

Ultimately, a face-centered central composite design appears best-suited for this investigation. This particular model discretizes each variable to three levels which are the extreme levels representative of the lower and upper bounds as described in Table 1, and a mid-level corresponding to a value bisecting the bounds. The selected face-centered model will account for any potential curvature in the system while providing a good coverage of the design space with a minimal set of data points. A standard central composite design, similar in form to the face-centered model but producing an equidistant distribution of data points, was found inappropriate for this study. In this particular response surface, the axial points would reside sufficiently outside the scope of the variable bounds so as to produce inefficient or infeasible wing designs. Table 3 summarizes all response surfaces considered and the number of experimental trials required.

Table 3 Required number of trials for various Design of Experiments.

Design of Experiments	Number of Required Trials
Full Factorial (2-Levels)	128
Full Factorial (3-Levels)	2187
Central Composite Design	143
Face-Centered Central Composite Design	143

EQUATION FORMULATION AND DATA REDUCTION

The functional form of a conventional wing weight equation will initially be used as a basis on which to build the new function. For example, consider the following conventional form taken from Ref. 6:

$$W_{Wing_{Conv.}} = a_0 \frac{S^{a_1} AR^{a_2} M_H^{a_3} \left(W_0 n_{\max}\right)^{a_4} \lambda^{a_5}}{\left(100\, t/c\right)^{a_6} \left(\cos \Lambda\right)^{a_7}}$$

Here, a_i represent the unknown coefficient and exponents to be determined from a regression of a database of wings, n_{max} the maximum load factor, M_H the highest Mach number, and W_0 the takeoff weight of the aircraft. Multiplying the conventional form by a function of morphing parameters will result in an equation capable of approximating the response of the experimental data points:

$$W_{wing_{morphing}} = W_{wing_{conventional}} \times f\left(\Delta b, \Delta AR, \Delta S, \text{etc.}\right)$$

With a functional form for the morphing parameters, all unknown exponential coefficients in the equation will be determined using a least squares regression technique to match the ASTROS-generated results. The total variance produced over the response surface, as well as the equation's ability to accurately predict data within the design space (but not included in the regression), will be used as a metric of performance. A multiobjective approach will be undertaken to select the best functional form if the results do not clearly indicate an optimal equation.

INVESTIGATION AND EXPECTED RESULTS

Currently, data has been acquired for a nine-trial D-optimal set of experiments selected from the full composite model. This set of nine experiments provides a saturated design if a linear least-squares routine were employed. The functional form ($\Delta b/b$) was selected to demonstrate the entire regression process, so the resulting morphing wing weight equation is:

$$W_{wing_{morphing}} = a_0 \frac{S^{a_1} AR^{a_2} M_H^{a_3} \left(W_0 n_{max}\right)^{a_4} \lambda^{a_5}}{\left(100\, t/c\right)^{a_6} \left(\cos \Lambda\right)^{a_7}} \left(\frac{\Delta b}{b}\right)^{a_8}$$

Using a nonlinear least squares regression algorithm, the leading coefficient and eight unknown exponents were determined to be as follows

$$W_{Wing_{Telescopic}} = 0.0474 \frac{S^{-0.0716} AR^{0.2353} M_H^{1.0104} \left(W_0 n_{max}\right)^{0.7911} \lambda^{-0.2678}}{\left(100\, t/c\right)^{-0.1666} \left(\cos \Lambda_{LE}\right)^{9.2729}} \left(\frac{\Delta b}{b}\right)^{0.2645}$$

This equation results in a residual norm of 3.726×10^4 lb^2. Given the optimal wing weights range from approximately 900 to 1600 pounds for the geometries analyzed, the residual obtained using Equation 5 would correlate to an error of 60 pounds at every data point (assuming the error is evenly distributed over the response surface). This seems to indicate a fairly good fit to the available data; however, the relative performance of this equation can not be ascertained since no other approximations have yet been derived. Additionally, the morphing wing weight predictor seems to have a few important, non-intuitive aspects. Most notable in these non-intuitive aspects are that the equation suggests a reduction in wing weight for an increase in wing area and a decrease in weight for a decrease in thickness-to-chord ratio. It is possible that these trends do exist for the non-traditional telescoping concept for morphing; however, given the very small number of data points used to build the above equation, confidence in the predictions is low.

At the end of the grant period, work was underway to complete all experimental trials from the central composite design set. Future work to include an investigation of the various functional forms for the wing weight equation would be of significant benefit. The method used to develop the wing weight predictor for the telescoping wing concept could readily be followed for other morphing strategies – including, but not limited to, the out-of-plane folding and the sweeping / sliding concepts being pursued by the DARPA MAS performers. With computational databases, morphing wing weight predictors could be developed specifically for each morphing concept. Additionally, the set of databases for several different morphing concepts might lead to a more generic morphing wing weight equation that could be used in very early morphing aircraft studies where the specific morphing concept is not yet defined.

Because this work to develop weight predictor equations relies upon computational analysis and optimization, an appropriate optimization approach is needed for morphing wings. The current approach uses separate optimization runs for each wing configuration, as described above. The results are then combined taking the larger element / component thickness from all results as the thickness used in the

design. This approach leads to designs where the load path for one geometric configuration can be notably different from the load path for another geometric configuration. An alternate approach that evaluates all geometric configurations and loading conditions in the same optimization problem may encourage designs that have lower total weight by sharing load paths among the geometric configurations. To do this, the optimization approach needs to appropriately address this. Also, the flutter analyses used in each separate optimization does not provide any information about the aggregate solution, so that flutter of the final design in either configuration is not truly used as a constraint. The Purdue team would like to investigate and develop an approach in which one optimization function evaluation may use a structural analysis for each geometric configuration. ASTROS would continue to serve as the analysis tool; this should allow for a better structural optimization result in which load paths may be shared where appropriate and will have consistent flutter analyses.

DOCUMENTATION

This topic was the most recent topic undertaken during the research period; as a result, documentation for this will appear shortly in the following conference paper and thesis.

Skillen, M., Newsome, E., and Crossley, W., "Developing Response Surface Based Wing Weight Equations for Conceptual Morphing Aircraft Sizing," to be presented at the 13th AIAA/ASME/AHS Adaptive Structures Conference, Apr. 2005.

Skillen, M., "Morphing Wing Weight Estimation Using Aeroelastic Optimization and Response Surface Methods," M.S. Thesis, School of Aeronautics and Astronautics, Purdue University, West Lafayette, IN, anticipated May 2005.

TECHNOLOGY TRANSFER

The first investigations conducted under this effort focused upon joined-wing aircraft concepts. Several joined-wing concepts have been proposed over the past several years, including the high-altitude, long-endurance "sensorcraft" concept developed within AFRL. The work pursued under this effort included the identification of body-freedom flutter as an important consideration, which has been cited in several different discussions of joined wing aircraft.

The more recent work dealing with morphing aircraft, particularly the weight estimation and structural optimization efforts, is aligned with the current DARPA Morphing Aircraft Structures program. Engineers from the two major performers under the DARPA program, Lockheed Martin and NextGen Aeronautics, have regularly been exchanging information with the Purdue PI and his research assistants regarding the approaches for modeling and structural optimization of morphing wings. Tentatively, it is planned to send a graduate research assistant that was supported by this effort from Purdue University to Lockheed-Martin for the Summer of 2004 to continue related investigations for morphing wings.

CONCLUDING REMARKS

The work described in this document made use of several computational analyses along with optimization methods to develop and investigate several approaches needed for the design of two types of advanced aircraft – joined-wing aircraft and morphing aircraft.

The investigations for the joined wing concepts identified body-freedom flutter as an important design consideration for this type of aircraft. Methods to predict the transition between body-freedom flutter mode and wing-cantilever flutter as the critical mode were also developed and demonstrated.

The study of wings with integrated conformal control surfaces demonstrated that the effects of the wing planform on wing structural weight, induced drag and control work (energy needed) present potentially competing objectives. The approaches developed indicate how multiobjective optimization methods could be applied to identify the best possible tradeoffs among these design objectives.

Approaches for aeroelastic analysis of two types of morphing wings, a telescoping wing and an out-of-plane folding wing, were developed and presented. This work demonstrated the importance of the layout of the wing on aeroelastic response for both the telescoping wing and the folding wing.

An investigation of using energy as an objective for design of morphing airfoils and wings was a more recent portion of the total improved methodology effort. The necessity to determine a tradeoff between actuation energy and aerodynamic performance motivated this work. While additional work is still necessary to realize the potential this approach offers, the results obtained here indicate that the tradeoffs between energy and efficiency to exist and that there are appropriate multiobjective optimization approaches to identify these optimal tradeoffs.

The investigation of predicting morphing wing weight using computational analyses and a design of experiments approach also would benefit from additional effort. While trying to develop a wing weight predictor, this effort also uncovered important issues for structural optimization of a morphing wing loaded under multiple geometric configurations. At the end of this effort, a small number of computational experiments had been completed and a first attempt at generating an estimating equation for morphing wing weight was made. Further studies of both the optimization approach and of the design of experiments-based technique to develop the weight equation would greatly improve the efficacy of these approaches for morphing aircraft design.

As a result of this effort, seven graduate research assistants and one post-doctoral associate were supported. One PhD thesis and two MS theses were completed during the grant period, and one PhD thesis and two MS theses are currently in progress based upon work begun under this effort. Five conference papers have been presented about this work, and two more will be presented at AIAA conferences in the near future. Subsequent journal submission of at least two articles is planned.